EARTHQUAKE ENGINEERING AND STRUCTURAL DYNAMICS
Earthquake Engng Struct. Dyn. 2007; **36**:307–325
Published online 12 September 2006 in Wiley InterScience (www.interscience.wiley.com). DOI: 10.1002/eqe.632

Damage-based design with no repairs for multiple events and its sensitivity to seismicity model

S. Das[‡], V. K. Gupta[*,†] and V. Srimahavishnu[§]

Department of Civil Engineering, Indian Institute of Technology Kanpur, Kanpur 208016, India

SUMMARY

Conventional design methodology for the earthquake-resistant structures is based on the concept of ensuring 'no collapse' during the most severe earthquake event. This methodology does not envisage the possibility of continuous damage accumulation during several not-so-severe earthquake events, as may be the case in the areas of moderate to high seismicity, particularly when it is economically infeasible to carry out repairs after damaging events. As a result, the structure may collapse or may necessitate large scale repairs much before the design life of the structure is over. This study considers the use of design force ratio (DFR) spectrum for taking an informed decision on the extent to which yield strength levels should be raised to avoid such a scenario. DFR spectrum gives the ratios by which the yield strength levels of single-degree-of-freedom oscillators of different initial periods should be increased in order to limit the total damage caused by all earthquake events during the lifetime to a specified level. The DFR spectra are compared for three different seismicity models in case of elasto-plastic oscillators: one corresponding to the exponential distribution for return periods of large events and the other two corresponding to the lognormal and Weibull distributions. It is shown through numerical study for a hypothetical seismic region that the use of simple exponential model may be acceptable only for small values of the seismic gap length. For moderately large to large seismic gap lengths, it may be conservative to use the lognormal model, while the Weibull model may be assumed for very large seismic gap lengths. Copyright © 2006 John Wiley & Sons, Ltd.

Received 11 February 2006; Revised 11 May 2006; Accepted 31 July 2006

KEY WORDS: cumulative damage; design force ratio spectrum; performance-based design; seismicity model; order statistics; hazard function

[*]Correspondence to: V. K. Gupta, Department of Civil Engineering, Indian Institute of Technology Kanpur, Kanpur 208016, India.
[†]E-mail: vinaykg@iitk.ac.in
[‡]E-mail: sandip@iitk.ac.in
[§]E-mail: S.vinjamuri@lycos.com

1. INTRODUCTION

As per the existing philosophy of aseismic design, a structure is designed for no collapse during the most critical earthquake expected at the given site. The evolution of performance-based design over the past decade has seen adding up of a few more performance levels in order to ensure that the structure also remains functional after a moderately strong event. Still, the possibility remains that in case of multiple earthquake events expected during the design life of the structure, the structure gets gradually damaged because it may be infeasible to carry out repairs after every event that drives structural response into the inelastic range. The smaller events may even damage the structure and render it unusable well before its design life is over, unless large scale repairs are carried out leading to interruption of business activity and thus to heavy financial losses. In an alternate scenario, these events may weaken the structure to the extent that it can no longer survive the most critical event. The design force level should therefore be so chosen that the damage likely to be experienced by the structure by the end of its design life is limited to a level acceptable to its owner.

There has been little effort in the direction of evaluating seismic performance of structures during multiple events over a period of time. In a recent study, Amadio *et al.* [1] analysed the effects of repeated earthquake ground motions on single-degree-of-freedom (SDOF) systems with non-linear behaviour and showed that under repeated earthquake ground motions there was a significant reduction in q factor (q factor is defined as the scale factor that should be applied to the accelerogram that produces first yielding somewhere in the structure, in order to obtain the maximum accelerogram that the structure can withstand without failure [2, 3]). However, they simulated repeated events via repetitions of identical accelerograms, which is not compatible with any realistic seismic environment.

The choice of a proper seismicity model is crucial to a study focussed on the effects of multiple earthquake events. Seismicity of a region represents the rates of occurrence of earthquakes of different magnitudes in that region. The magnitude–frequency relationship given by Gutenberg and Richter [4] is widely used to estimate the expected number of earthquake occurrences above a given magnitude interval. Such estimation is, however, independent of the time distribution followed by these occurrences.

Several researchers have attempted to devise analytical models for earthquake occurrences. Many early models assumed that occurrences of earthquake events constitute a Poisson process and that the return period for these events is exponentially distributed. These models thus correspond to constant hazard function. The Poisson process is not physically unreasonable for events of small to medium magnitudes [5]. Further, as the combination of several non-Poissonian processes can be approximated as a Poisson process, a Poissonian model may also be acceptable when dealing with occurrences of large earthquakes on a global level. However, because of the memoryless nature of a Poisson process, the probability of an event occurring during a given exposure time does not depend on the history of past occurrences. On the other hand, physical models of gradually accumulated and suddenly released energy call for a process such that the waiting time for the next event decreases with the time elapsed since the last event [6]. Patwardhan *et al.* [7], Kiremidjian and Suzuki [8], Cornell and Winterstein [5] have, therefore, suggested semi-Markov models with a time-dependent hazard function based on lognormal or Weibull distributions of return period.

In the models assuming lognormal or Weibull distribution of return periods, as the hazard functions are time-dependent, the number of occurrences in a given period of time depends on the knowledge of the time of occurrence of the last event. These models have been found to well

DOI: 10.1002/eqe

represent the occurrences of large earthquakes of many regions (see References [5, 9]). However, there are several regions for which the statistical evidence to support seismic gap and characteristic earthquake hypothesis is inadequate [10]. For such regions, it is very difficult to find the seismicity model that best fits with the statistical data.

Besides properly modelling the seismicity of the region, it is important to estimate the magnitudes of all earthquake events expected to occur in a given period of time. Chen and Lin [11], Kijiko and Sellovel [12], Yegulalp and Kuo [13] have obtained different extreme value distributions to evaluate the largest earthquake magnitude for a given period and for a given confidence level. Gupta and Despande [14] have shown that Log-Pearson Type-III distribution can be used to get very realistic estimates of largest earthquake magnitudes for different return periods. These distributions cannot, however, be used to estimate the magnitudes of second largest, third largest, etc. earthquakes.

Within the broad framework of performance-based design, this study looks at the effect of seismicity model on the factor by which the design yield force level of a conventionally designed SDOF structure should be increased in order to limit the cumulative damage during its life-time to a specified level. This is done by considering several elasto-perfectly plastic SDOF oscillators of different initial periods and by obtaining spectra of this factor, to be called as design force ratio (DFR), in case of three seismicity models. The three models consider different distributions for the return periods; in the first model, exponential distribution is assumed over the entire range of magnitudes, while in the second and third models, return periods of large earthquakes follow lognormal and Weibull distributions, respectively. Order statistics approach is used to estimate the expected magnitudes of ordered earthquake events, assuming that all events likely to occur in the given period of time are statistically independent. A hypothetical region consisting of four faults with different rates of occurrences is considered for a numerical study on the sensitivity of DFR spectrum to the seismicity model.

2. DFR SPECTRUM

The design force ratio (DFR) spectrum is defined to give the values of DFR, i.e.

$$\alpha_R = \frac{\bar{Q}_y}{Q_y} \tag{1}$$

for various SDOF oscillators of different initial periods, for a given combination of damping ratio, available ductility and (cumulative) damage level. In Equation (1), Q_y is the yield force level as obtained in the conventional design, and corresponds to the expected maximum displacement being consistent with the available ductility during the most critical or design earthquake event. $\bar{Q}_y$ is the yield force level required for the structure to undergo a specified level of expected cumulative damage during all earthquake events expected to occur in its lifetime. A value of α_R close to unity implies that the conventional design approach may be adequate at the given site for the structure to survive through its life-time (with the condition that no repairs are carried out after any event), whereas a much higher value than unity implies that such approach may lead to a significantly unsafe design of structure. It may be noted that α_R includes the effects of shift from the conventional (ductility-based) design to a damage-based design, besides including the effects of shift from single-event design to a multiple-event design.

Both Q_y and $\bar{Q}_y$ need to be estimated iteratively, for a given SDOF oscillator and seismic environment, such that those are, respectively, consistent with the specified values of available

DOI: 10.1002/eqe

ductility and cumulative damage. For convenience, this study considers the use of linear random vibration theory together with equivalent linearization of the (non-linear) oscillator for obtaining the largest peak response of the oscillator. Further, it is assumed for calculating $\bar{Q}_y$ that the same equivalent oscillator as used for obtaining the largest peak response can also be used for obtaining the second largest, third largest, etc. peak responses. The order statistics approach is assumed to be applicable for estimating the magnitudes of the largest and other events during the lifetime of the structure. Simplifying assumptions are also made regarding the strength and stiffness degradations in the oscillator during an event and regarding the sequence of occurrence of the damaging events. Following are the details of the procedure used in this study.

2.1. Estimation of power spectral density function

In using the linear random vibration theory, it is convenient to characterize the ground acceleration process for an event in terms of its power spectral density function (PSDF). As the direct scaling of PSDF has yet to become popular, the estimation of PSDF is done here by using the known relationships for scaling Fourier spectrum, strong motion duration, and peak ground acceleration (PGA) in terms of the parameters like earthquake magnitude, epicentral distance and geological site conditions.

Assuming the earthquake ground acceleration to be a stationary process, the PSDF corresponding to the M_k magnitude event occurring at the lth source is evaluated at frequency ω as

$$G_{lk}(\omega) = \frac{Z_{lk}^2(\omega)}{\pi T_{lk}} \tag{2}$$

where, $Z_{lk}(\omega)$ and T_{lk}, respectively, are the Fourier spectrum and strong motion duration of ground acceleration for the event of magnitude M_k occurring at the epicentral distance R_l. There is no unique or universally accepted definition of strong motion duration available yet. However, in consistency with Equation (4) used in this study for the purpose of scaling, the 90%-central-energy duration by Trifunac and Brady [15] is assumed to be applicable here. To include the effects of inherent non-stationarity in ground motion, $G_{lk}(\omega)$ is scaled up or down to $\bar{G}_{lk}(\omega)$ so as to correspond to the same expected PGA as that estimated by a suitable attenuation relationship (see Equation (5), for example). To include the effects of non-stationarity (in response) due to the sudden application of excitation, one may use the transient transfer function at a finite value of time-instant t (in place of the steady-state transfer function in the stationary random vibration theory), as reasoned by Gupta and Trifunac [16]. In this study, transient transfer function evaluated at $t = 0.2T_{lk}$ will be assumed to be uniformly applicable for the oscillators of all initial periods considered.

For the scaling of $Z_{lk}(\omega)$, a simple and convenient relationship as proposed by Trifunac and Lee [17] is used here. According to this relationship, the Fourier spectrum $\mathrm{FS}(T)$ may be expressed in terms of earthquake magnitude M, representative distance Δ from source to site, and geologic site condition s ($=0$ for alluvium, 1 for intermediate, and 2 for rock) as

$$\log_{10}\mathrm{FS}(T) = M + \mathrm{Att}(\Delta, M, T) + b_1(T)M + b_2(T)s + b_5(T) + b_6(T)M^2 + \varepsilon(p, T) \tag{3}$$

where $\varepsilon(p, T)$ is the observed residual spectrum for a given confidence level, p. In this study, $p = 0.5$ (for 50% confidence level) has been considered to get the median Fourier spectrum. The representative distance Δ is expressed in terms of the epicentral distance, focal depth, fault size

DOI: 10.1002/eqe

and coherence radius [17]. Further, b's represent the coefficients determined from a regression analysis at each period, T, and Att(Δ, M, T) represents the attenuation function [17].

For the scaling of T_{lk}, the relationship given by Trifunac and Brady [15] is used here. According to this relationship, the mean strong motion duration T_s may be expressed as

$$T_s = -4.88s + 2.33M + 0.149R \tag{4}$$

where R is the epicentral distance. Further, the following attenuation relationship given by Trifunac and Brady [18] is used for the estimation of mean PGA,

$$\log \mathrm{PGA} = M + \log A_0(R) - \log a(M) \tag{5}$$

where $A_0(R)$ represents the attenuation of acceleration with epicentral distance and $a(M)$ represents the magnitude-dependent scaling constant as determined by a regression analysis.

2.2. Equivalent linear oscillator and response statistics

Once the PSDF $\bar{G}_{lk}(\omega)$ is determined for an event of magnitude M_k, occurring at the lth source, the structural response to this event is estimated by replacing the given non-linear oscillator by an equivalent linear oscillator, multiplying $\bar{G}_{lk}(\omega)$ by the squared modulus of the response transfer function, and by using the order statistics approach on the response PSDF so obtained.

For an elasto-perfectly plastic SDOF oscillator of initial frequency ω_n, viscous damping ratio ζ and yield displacement x_y, the damping ratio ζ_e and natural frequency ω_e of the equivalent linear oscillator are given by Caughey [19]

$$\omega_e^2 = \omega_n^2 - \omega_n^2 g(\sigma_y) \tag{6}$$

$$\zeta_e = \frac{\zeta\omega_n}{\omega_e} + \frac{\omega_n^2}{\sqrt{2\pi}\omega_e^2\sigma_y}\left[1 - \mathrm{erf}\left(\frac{1}{\sqrt{2}\sigma_y}\right)\right] \tag{7}$$

with

$$\sigma_y = \frac{x_{\mathrm{rms}}}{x_y} \tag{8}$$

$$g(\sigma_y) = \frac{1}{2\pi\sigma_y^4}\int_1^\infty A^3\left(\pi - \Lambda + \frac{1}{2}\sin 2\Lambda\right)\exp\left(-\frac{A^2}{2\sigma_y^2}\right)\mathrm{d}A \tag{9}$$

and erf (.) representing the error function. In Equation (8), we have

$$x_{\mathrm{rms}} = \left[\int_0^\infty |\tilde{H}(\omega)|^2\bar{G}_{lk}(\omega)\,\mathrm{d}\omega\right]^{1/2} \tag{10}$$

where $\tilde{H}(\omega)$ is the transient transfer function $\tilde{H}(\omega, t)$ evaluated at $t = 0.2T_{lk}$. With ω_d ($=\omega_e\sqrt{1-\zeta^2}$) representing the damped natural frequency, the transient transfer function may be expressed as [16]

$$\tilde{H}(\omega, t) = \frac{1}{(\omega_e^2 - \omega^2) + 2i\zeta_e\omega_e\omega}\left[\mathrm{e}^{-\mathrm{i}\omega t} - \mathrm{e}^{-\zeta\omega_e t}\left(\cos\omega_d t + \frac{\zeta\omega_e - \mathrm{i}\omega}{\omega_d}\sin\omega_d t\right)\right] \tag{11}$$

DOI: 10.1002/eqe

In Equation (9), we further have

$$\Lambda = \cos^{-1}\left(1 - \frac{2}{A}\right) \tag{12}$$

The properties of the equivalent linear oscillator are obtained through an iterative process. With an initial guess of σ_y, the values of ω_e and ζ_e are obtained by using Equations (6) and (7), x_{rms} is obtained by using Equation (10), and then σ_y is updated by using Equation (8). After obtaining the linearized properties, ω_e and ζ_e, the response PSDF is calculated as

$$E_{lk}(\omega) = |\tilde{H}(\omega)|^2 \bar{G}_{lk}(\omega) \tag{13}$$

From this, the expected amplitude of the ith-order displacement response peak, i.e. $E[x_{(i)}]$, is evaluated as [20]

$$E[x_{(i)}] = \left[\int_0^\infty E_{lk}(\omega)\,\mathrm{d}\omega\right]^{1/2} \int_{-\infty}^{\infty} \eta p_{(i)}(\eta)\,\mathrm{d}\eta \tag{14}$$

where

$$p_{(i)}(\eta) = \frac{N!}{(N-i)!(i-1)!}[P(\eta)]^{i-1}[1 - P(\eta)]^{N-i} p(\eta) \tag{15}$$

is the probability density function of the ith-order peak. In Equation (15),

$$p(\eta) = \frac{1}{\sqrt{2\pi}}\left[\varepsilon \mathrm{e}^{-\eta^2/2\varepsilon^2} + (1-\varepsilon^2)^{1/2}\eta \mathrm{e}^{-\eta^2/2}\int_{-\infty}^{\eta(1-\varepsilon^2)^{1/2}/\varepsilon} \mathrm{e}^{-x^2/2}\,\mathrm{d}x\right] \tag{16}$$

and

$$P(\eta) = \int_\eta^\infty p(u)\,\mathrm{d}u \tag{17}$$

respectively, are the probability density and cumulative probability functions of the peaks in the displacement response process, and

$$N = \frac{T_{lk}}{2\pi}\left[\frac{\lambda_4}{\lambda_2}\right]^{1/2} \tag{18}$$

is the expected number of peaks in this process. In Equation (16), ε is the bandwidth parameter defined as

$$\varepsilon = \left[\frac{\lambda_0\lambda_4 - \lambda_2^2}{\lambda_0\lambda_4}\right]^{1/2} \tag{19}$$

where λ_n is, in general, the nth moment of the PSDF $E_{lk}(\omega)$, and is defined by

$$\lambda_n = \int_0^\infty \omega^n E_{lk}(\omega)\,\mathrm{d}\omega, \quad n = 0, 1, 2, \ldots \tag{20}$$

For the expected amplitude of the ith-order peak in the absolute response process, i.e. $E[|x|_{(i)}]$, $p(\eta)$ and N are taken as [21]

$$p(\eta) = \frac{\sqrt{2}}{\sqrt{\pi}(1+\sqrt{1-\varepsilon^2})}\left[\varepsilon \mathrm{e}^{-\eta^2/2\varepsilon^2} + (1-\varepsilon^2)^{1/2}\eta \mathrm{e}^{-\eta^2/2}\int_{-\infty}^{\eta(1-\varepsilon^2)^{1/2}/\varepsilon} \mathrm{e}^{-x^2/2}\,\mathrm{d}x\right] \tag{21}$$

DOI: 10.1002/eqe

and

$$N = \frac{T_{lk}}{2\pi}(1 + \sqrt{1 - \varepsilon^2}) \left[\frac{\lambda_4}{\lambda_2}\right]^{1/2} \tag{22}$$

instead of the expressions in Equations (16) and (18), respectively.

It may be mentioned that the properties of the equivalent oscillator obtained via Equations (6)–(12) are for the largest response peak, and therefore those may not be strictly applicable for estimating the second largest, third largest, etc. response peaks via the order statistics approach. Also, those do not account for the effects of degradation in stiffness or strength during the ground motion. For simplicity here, the resulting errors are assumed to be negligible. Further, the largest peak amplitude $E[|x|_{(1)}]$ computed above is for a chosen value of yield displacement x_y. In conventional earthquake-resistant design, x_y has to be so chosen (for Q_y) that $E[|x|_{(1)}]$ is equal to μx_y (μ is the available ductility) during the most critical earthquake event likely (at all faults) during the lifetime of the structure. In other words, x_y is the lowest yield displacement in order for $E[|x|_{(1)}]$ not to exceed μx_y during each of the events expected during the lifetime of the structure. In damage-based design, x_y has to be chosen at a higher level (for $\bar{Q}_y$) so that the oscillator undergoes a specified amount of damage on being subjected to $E[|x|_{(1)}]$, $E[|x|_{(2)}]$, ..., $E[|x|_{(N)}]$ response peaks during each of the events expected in the lifetime of the structure.

2.3. Damage during single event

For the calculation of $\bar{Q}_y$, it is necessary to estimate the damage to which the oscillator of given initial period, damping ratio, and yield displacement x_y will be subjected during the event of magnitude M_k at the lth source. This is estimated here as [22]

$$D_{lk} = \frac{x_m - x_y}{x_u - x_y} + \beta \frac{EH}{Q_y x_u} \tag{23}$$

where x_m ($= E[|x|_{(1)}]$) is the expected maximum displacement that the equivalent linear SDOF system would undergo during the base excitation, x_u ($= \mu x_y$) is the ultimate displacement of the system under monotonic loading, β represents the effect of cyclic loading on structural damage, EH represents the total energy dissipation in the structure during the excitation, and Q_y is the lateral force at which first yielding of the structure takes place. Damage D_{lk} is zero when x_m does not exceed x_y.

Assuming the response to be a narrow-band process and taking $\beta = 0.1$, the damage D_{lk} is obtained as

$$D_{lk} = \frac{E[|x|_{(1)}] - x_y}{x_u - x_y} + 0.1 \frac{\sum_{i=1}^{N_0} 4(E[x_{(i)}] - x_y)}{x_u} \tag{24}$$

where N_0 is the total number of positive zero crossings given by

$$N_0 = \frac{T_{lk}}{2\pi}(1 + \sqrt{1 - \varepsilon^2}) \left[\frac{\lambda_2}{\lambda_0}\right]^{1/2} \tag{25}$$

2.4. Cumulative damage

After the damage during each of the events expected in the design life of the structure is estimated, the cumulative damage in that period is estimated by adding individual damages caused by those

DOI: 10.1002/eqe

events. Since there is a degradation in stiffness and strength during each damaging event, the value of x_y to be used in Equation (24) would be the value of yield displacement of the oscillator just before the occurrence of the event, and the cumulative damage will depend much on the sequence in which the damaging events occur. This study considers the most conservative estimate of the cumulative damage, and therefore, all anticipated events are assumed to take place in the descending order of the damage they would inflict on the just-built structure. As the events that cause no damage to the undamaged structure may still cause some damage to the structure with degraded strength and stiffness, those are assumed to take place in the descending order with respect to the maximum displacement of the just-built structure. During each damaging event, the strength and stiffness of the structure are assumed to degrade as explained below.

It is assumed that the yield displacement $x_{y,i}$ increases after the ith damaging event to $x_{y,i+1}$, such that

$$x_{y,i+1} = \left(\frac{k_1 + k_i}{k_1 + k_{i+1}}\right) x_{y,i} \tag{26}$$

Here, k_1 denotes the initial stiffness of the system, and k_i and k_{i+1}, respectively, denote the stiffness of the system before and after the ith event. Equation (26) is based on the assumption that the maximum increase in the yield displacement is equal to $x_{y,1}$ $(= x_y)$ in the case of complete degradation of the stiffness. Also, it may be observed that $x_{y,i+1} = 2x_y$ when $k_i = k_1$ and $k_{i+1} = 0$. Further, considering the stiffness degradation to be an increasing function of the maximum displacement beyond the yield displacement during the ith damaging event, the stiffness k_{i+1} is assumed as

$$k_{i+1} = k_i \left[1 - \frac{E[|x|_{(1),i}] - x_{y,i}}{x_u - x_{y,i}}\right]^{\gamma} \tag{27}$$

Here, $|x|_{(1),i}$ and $x_{y,i}$, respectively, represent the values of $|x|_{(1)}$ and x_y during the ith damaging event. Further, the parameter, γ, is taken arbitrarily as 0.1 considering the degradation in the moment capacity of the reinforced concrete members as modelled by Reinhorn *et al.* [23]. The strength degradation is assumed to be governed by the stiffness degradation as in Equation (27) and by the increase in yield displacement as in Equation (26). It is also assumed that the structure does not undergo any repairs after any damaging event and thus, the strength and stiffness of the structure after the ith event are same as the strength and stiffness of the structure before the $(i + 1)$th event.

3. SEISMICITY MODELLING AND EXPECTED MAGNITUDES OF EARTHQUAKE EVENTS

3.1. Seismicity modelling

For the calculation of the cumulative damage due to various seismic events, it is necessary to know the number of events of different magnitudes that are likely to occur at each of the faults in a given time-window. Let the seismicity of each contributing fault be known apriori in terms of the rates of occurrences of earthquakes of different magnitudes. Further, let the average rate of occurrence per year, N_l, of the earthquakes of magnitude M and higher at the lth source be described by the Gutenberg–Richter relationship as

$$\log N_l = a_l - b_l M \tag{28}$$

DOI: 10.1002/eqe

where a_l and b_l are constants estimated from the catalog of past earthquakes or from the known slip rate at the lth source. If all the events of magnitude M and higher at a source are assumed to follow a Poissonian sequence of occurrences, $1/N_l$ would represent the mean return period of occurrence of those events. It is not, however, realistic to assume a uniform rate of occurrence for the large earthquakes that may completely rupture the fault or fault segment under consideration. The likelihood of occurrence has to vary with the quiescent period or the period of strain build-up since the last such event. Hence, the return period should be distributed based on how much time has elapsed since the occurrence of the last characteristic event on the source under consideration. This calls for the use of a time-dependent hazard function such as that based on the lognormal or Weibull distribution of return period. If $f(t)$ represents the probability density function of the return period and $F(t)$ represents the corresponding cumulative probability distribution, the hazard rate

$$h(t) = \frac{f(t)}{1 - F(t)} \tag{29}$$

would represent the number of events in the time interval, $(t, t+\mathrm{d}t)$. For a Poissonian distribution of earthquake occurrences, the return period follows exponential distribution, and then, the hazard rate is constant (irrespective of the length of quiescent period) and equal to the number of occurrences per unit time.

As discussed in Section 1, the return period of large earthquakes may be considered to follow either lognormal or Weibull distribution. In case of lognormal distribution, the hazard rate at the lth source may be written as

$$h_l(t) = \frac{\phi\left[\dfrac{\ln t - \lambda_l}{\zeta_l}\right]}{\zeta_l t\left(1 - \Phi\left[\dfrac{\ln t - \lambda_l}{\zeta_l}\right]\right)} \tag{30}$$

where λ_l and ζ_l are, respectively, the mean and standard deviation of the random variable, $\ln T_l$, with T_l denoting the return period of the large earthquakes. Further, $\phi(.)$ and $\Phi(.)$, respectively, are the standard normal density and distribution functions. The value of ζ_l is taken here equal to 0.2 as in Todorovska [24]. This is close to the generic value of 0.215, as obtained by Nishenko and Buland [9] from a large set of data, for the standard deviation of $\ln T/\tilde{T}$ where $\tilde{T}$ is the median of the return period. For a meaningful comparison of different seismicity models, it is desirable to keep the means of various distributions of return period equal. Then, it can be shown that (see Reference [24] for example)

$$\lambda_l = -\ln N_l - \zeta_l^2/2 \tag{31}$$

When the return periods follow Weibull distribution, the hazard rate at the lth source can be shown to be [5]

$$h_l(t) = \frac{(V_{T_l} - 1)!}{\mu_{T_l}}\left(\frac{V_{T_l}!t}{\mu_{T_l}}\right)^{(1-V_{T_l})/V_{T_l}} \tag{32}$$

where $\mu_{T_l} = 1/N_l$ is the mean value and V_{T_l} is the coefficient of variation of return period. In this study, the value of V_{T_l} is taken as 0.3 for a strongly characteristic behaviour and in consistency with the values reported for various regions [5, 25].

DOI: 10.1002/eqe

Given that there are no events in T_0 years since the last event, the expected number of occurrences of large earthquakes at the lth source in the next Y years is given by

$$N_l(T_0 + Y|T_0) = \int_{T_0}^{T_0+Y} h_l(\tau)\,\mathrm{d}\tau \tag{33}$$

In this study, the earthquakes of 7 and higher magnitudes are considered to imply large earthquakes. Such earthquakes rupture the fault so extensively that once an event in this magnitude range occurs, it takes considerable time for another event of the same or higher magnitude to occur.

As mentioned in Section 1, there is a large uncertainty regarding the earthquake events that are likely to occur at a given fault of known seismicity, and therefore, three different seismicity models are considered in this study. In the first model, return period is assumed to follow exponential distribution over the entire range of magnitudes. In the second and third models, exponential distribution is assumed for the events up to the magnitude of 7. For the magnitudes between 7 and 8, lognormal distribution is assumed in case of the second model and Weibull distribution in case of the third model. All events below magnitude 5 are neglected, while it is assumed that no event with magnitude $M>8$ will occur. Thus, the expected total number of events $\tilde{N}$ in Y years is computed from Equation (28) (for $5 \leqslant M \leqslant 8$) in case of the first model, while it is obtained by adding the expected number of events computed from Equation (28) (for $5 \leqslant M<7$) and that from Equation (33) (for $7 \leqslant M \leqslant 8$) in case of the second and third models. For all three models, the method of truncation is used to round off $\tilde{N}$ to the next lower integer.

In case of the second and third models with time-dependent hazard function, the number of earthquakes as given by Equation (33) can be evaluated for different values of T_0. It can be shown that the hazard function based on Weibull distribution continuously increases with seismic gap length T_0 and gives quite unrealistic values as T_0 increases beyond certain level. On the other hand, hazard function for a lognormal distribution decreases continuously after increasing to its maximum.

3.2. Expected magnitudes of earthquake events

Once the expected number of earthquakes is calculated for a fault, the maximum magnitude during a given number of years may be estimated for a confidence level by the extreme event analysis. However, there exists no methodology at present to estimate the magnitudes of the second largest and higher order events. We therefore assume for this study that the events likely to occur at a fault over a given period of time are statistically independent and that the order statistics approach may be used to estimate the magnitudes of ordered events. The expected value of the magnitude of the ith largest event is thus estimated as

$$E[M_i] = \int_{M_{\min}}^{M_{\max}} m p_i(m)\,\mathrm{d}m \tag{34}$$

where

$$p_i(m) = \frac{\tilde{N}!}{(\tilde{N}-i)!(i-1)!}\,[F(m)]^{i-1}[1-F(m)]^{\tilde{N}-i}\,p(m) \tag{35}$$

is the probability density function of the ith largest event. In Equation (35), $\tilde{N}$ is the expected number of events in Y years in the range $M_{\min}$ $(=5)$ to $M_{\max}$ $(=8)$, and

$$F(m) = \mathrm{Prob}(M \geqslant m) = \frac{N(m) - N(M_{\max})}{N(M_{\min}) - N(M_{\max})} \tag{36}$$

DOI: 10.1002/eqe

and

$$p(m) = -\frac{\mathrm{d}F(m)}{\mathrm{d}m} \tag{37}$$

respectively, are the probability distribution and density functions of $\tilde{N}$ events in case of the models with time-dependent hazard rates. Here, $N(m)$ is the expected number of events in Y years in the range $[m, M_{\max}]$; and $p(m)$ is evaluated numerically by the finite-difference method. For the model with constant hazard rate, the number of earthquakes over the entire magnitude range are estimated from the Gutenberg–Richter relationship, and thus Equations (36) and (37), respectively, lead to

$$F(m) = \frac{10^{-b(m-M_{\min})} - 10^{-b(M_{\max}-M_{\min})}}{1 - 10^{-b(M_{\max}-M_{\min})}} \tag{38}$$

and

$$p(m) = b \ln 10 \frac{10^{-b(m-M_{\min})}}{1 - 10^{-b(M_{\max}-M_{\min})}} \tag{39}$$

The above procedure of estimating ordered earthquake events may be applicable only if no aftershocks are included in $\tilde{N}$. Aftershocks following an earthquake event generally constitute a sequence of events of decreasing magnitudes, with $F(m)$ for each of those events governed by the magnitude of the main event. It may be possible to extend the present analysis to include the effects of aftershocks by estimating their number and distribution and then by determining their ordered magnitudes independently for each of the main events. However, this is beyond the scope of this paper and the present study is only for those cases where the main events are followed by the non-damaging aftershocks.

4. NUMERICAL STUDY

4.1. The seismic environment

For the purpose of studying the sensitivity of DFR spectrum to seismicity model, a hypothetical seismic environment with faults of known parameters, a and b, has been considered in this study. This seismic environment is based on that considered by Todorovska [24] and consists of four faults: two faults located at a distance of 30 km each from the site, and the other two located at 40 and 50 km each. The values of a_l for these faults are taken as 3.28, 4.03, 3.77 and 3.09, respectively, while b_l has been assumed to be uniformly equal to 0.86 for all the four faults. The focal depths of the sources are assumed to be uniformly equal to 5 km, and the area under consideration is assumed to have alluvium geologic site conditions.

4.2. Results and discussion

For the construction of DFR spectrum (i.e. plot of α_R with the initial period of the SDOF oscillator), twenty elasto-perfectly plastic oscillators with initial periods of 0.1, 0.15, 0.2, 0.25, 0.3, 0.4, 0.5, 0.6, 0.75, 0.9, 1.0, 1.1, 1.25, 1.5, 1.75, 2.0, 2.5 s and uniform damping ratio of 5% are considered. The DFR spectrum is constructed for each of the three different seismicity models described in Section 3, and for a design life $Y = 50$ years. The value of Q_y in each case is determined by considering the lowest yield strength such that the expected maximum displacement of the

DOI: 10.1002/eqe

equivalent linear oscillator does not exceed μx_y during the largest magnitude event expected (for $i=1$ in Equation (34)) at each of the four faults during the lifetime of the structure. The value of $\bar{Q}_y$ is estimated by following the damage-based procedure for multiple events as outlined in the previous two sections. In case of the second and third models, the DFR spectrum is constructed for $T_0=0$, $0.5\mu_{T_l}$, μ_{T_l} and $1.5\mu_{T_l}$, with T_0 and μ_{T_l} as defined in the previous section. The values of α_R in each spectrum are estimated as the nearest multiples of 0.005.

The expected number of events is obtained as 4 with the magnitudes 6.03, 5.54, 5.24 and 5.13 in case of the first seismicity model for the fault having $a=3.28$. For the second seismicity model, this becomes 5 (4.68 for $5 \leqslant M<7$ plus 0.38 for $7 \leqslant M \leqslant 8$) with magnitudes 6.45, 5.78, 5.45, 5.25 and 5.11, and for the third seismicity model, this becomes $(4.68+0.20=)$ 4 with magnitudes 6.16, 5.58, 5.31 and 5.13, in case of $T_0=\mu_{T_l}$. For the fault having $a=4.03$, the numbers of events are 26 (largest magnitude = 6.84), 29 (largest magnitude = 7.48) and 28 (largest magnitude = 7.29) for the three seismicity models, respectively. For the fault with $a=3.77$, those are 14, 15 and 15, respectively (with the largest magnitudes of 6.57, 7.17 and 6.93), and for the fault with $a=3.09$, those are 3 for each of the seismicity models (with the largest magnitudes of 5.91, 6.14 and 6.01, respectively).

Figure 1 shows the DFR spectra for $\mu=2$, 2.5 and 3 in case of the seismicity model with exponentially distributed return period and cumulative damage level $D=0.8$ (see the curves without cross symbols). It is assumed that $D=0.8$ is representative of large damage without collapse as envisaged in the traditional seismic design for the most critical event. Figure 1 also shows the strength reduction factor R_μ values for the three ductility levels (see the curves with cross symbols). R_μ here refers to the ratio of the required yield strength for unit ductility demand to that for μ ductility demand in the given seismic environment. If the most critical events are identical for the elastic and inelastic responses, R_μ would become same as the conventional strength reduction factor. It may be observed that α_R increases with increasing ductility for a given initial period of oscillator but for a given ductility ratio, this remains below R_μ. As will be shown in Figure 2, the α_R curve takes higher values for lower D values. At $D=0$, the maximum displacement may not

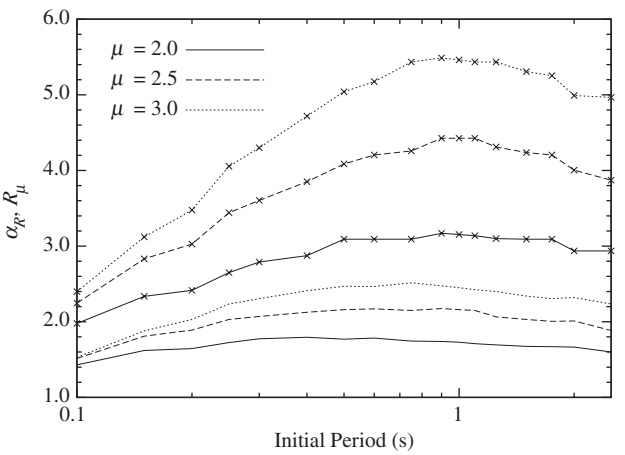

Figure 1. DFR spectra (without cross symbols) and R_μ spectra (with cross symbols) for different values of ductility ratio μ in case of $D=0.8$ and exponential seismicity model.

DOI: 10.1002/eqe

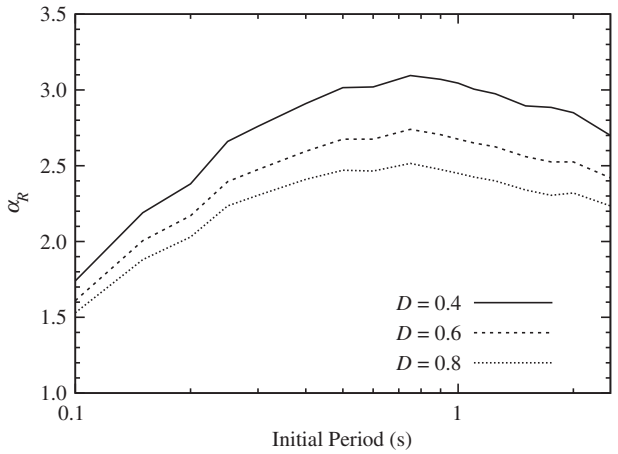

Figure 2. DFR spectra for different values of cumulative damage D in case of $\mu = 3$ and exponential seismicity model.

exceed the yield displacement under the most critical excitation and then α_R would become same as R_μ. It is obvious from Figure 1 that (conventionally designed) more ductile structural systems may be more susceptible for not surviving through the design life of the structure than the less ductile systems. This is because the conventional design approach envisages greater reductions in yield strength levels for more ductile systems, leading to higher damage levels and thus leaving little margins for surviving the other events.

Figure 2 shows the DFR spectra for (cumulative) damage levels of $D = 0.4$, 0.6 and 0.8 in case of the seismicity model with exponentially distributed return period and $\mu = 3$. Additional damage levels of 0.4 and 0.6 here represent the cases of moderate and significant damages in the structure, respectively. Though these damage levels are not consistent with the desired state of structure at the end of its design life, Figure 2 clearly shows the effect of damage level on the DFR spectrum. As expected, α_R increases with decrease in the damage level for a given oscillator period. It may be observed from Figure 2 that the yield levels obtained from the conventional design are not good enough for the multiple-event design, particularly when we aim for cumulative damage much less than that for collapse. Those may however be acceptable when the seismic environment becomes much milder than that considered in the example case here. This is illustrated in Figure 3 where DFR spectra for $\mu = 3$ and $D = 0.8$ are compared for three seismicity levels: (i) 'Seism1' for the seismicity level of the example case, (ii) 'Seism2' for the seismicity level corresponding to 50% of the earthquake occurrences in 'Seism1', and (iii) 'Seism3' for 5% of the earthquake occurrences in 'Seism1'. The cases of 'Seism2' and 'Seism3' have been obtained by taking the values of a_l as (2.98, 3.73, 3.47, 2.79) and (1.98, 2.73, 2.47, 1.79), respectively. It may be mentioned that the case of 'Seism3' effectively corresponds to single-event design. However, the α_R levels here are not close to unity because α_R includes the effects of shift from ductility-based to damage-based design. The effects of this shift can be made negligible by choosing a suitably higher value of D than 0.8.

Figures 4–7 show the comparisons of DFR spectra for the three seismicity models, in case of the seismicity gaps of 0, $0.5\mu_{T_l}$, μ_{T_l} and $1.5\mu_{T_l}$, respectively. Figures 8 and 9 respectively show the

DOI: 10.1002/eqe

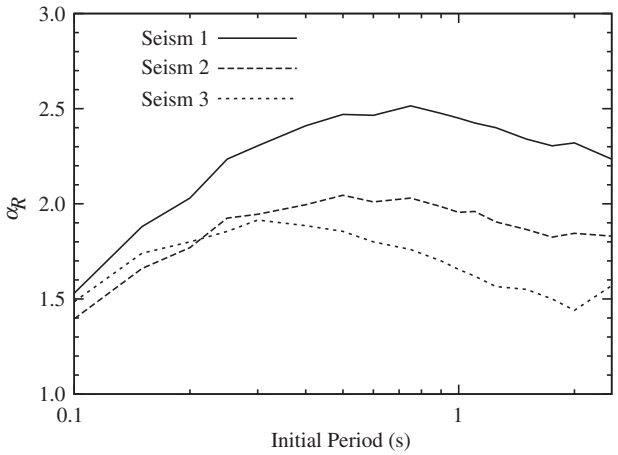

Figure 3. DFR spectra for different levels of seismicity in case of $\mu = 3$, $D = 0.8$, and exponential seismicity model.

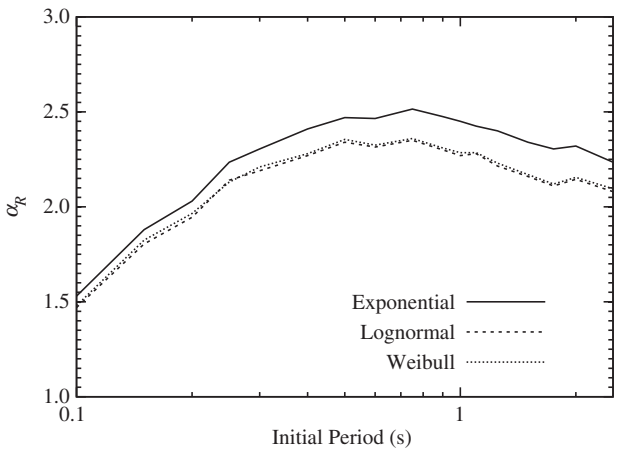

Figure 4. DFR spectra for different seismicity models in case of $\mu = 3$, $D = 0.8$, and $T_0 = 0$.

variations of single-event yield force Q_y and multiple-event yield force $\bar{Q}_y$ (as normalized with respect to mass) with T_0/μ_{T_l} for the three seismicity models in case of $\mu = 3$, $D = 0.8$, and 0.3 s oscillator. It may be observed from Figures 8 and 9 that the values of Q_y and $\bar{Q}_y$ corresponding to the exponential model are greater than those for the lognormal and Weibull models when T_0 is equal to zero. This is because hazard rate in case of the lognormal and Weibull models is lowest soon after an event, leading to greater expected value of the largest event and the number of events causing inelastic excursions for the exponential model. The effect of higher hazard rate is however observed more in case of $\bar{Q}_y$ (than Q_y) since $\bar{Q}_y$ is also influenced by the magnitudes of the second largest, third largest, etc. events, which increase with the total number of events. Figure 4

DOI: 10.1002/eqe

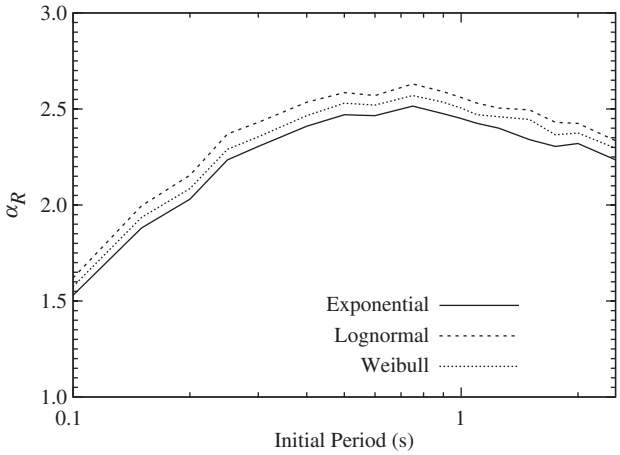

Figure 5. DFR spectra for different seismicity models in case of $\mu = 3$, $D = 0.8$, and $T_0 = 0.5\mu_{T_l}$.

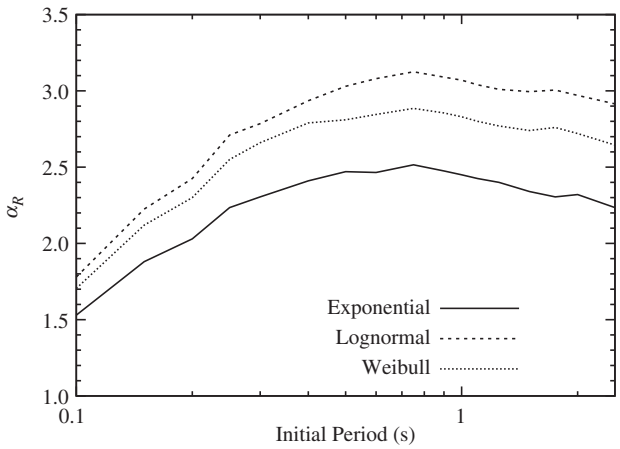

Figure 6. DFR spectra for different seismicity models in case of $\mu = 3$, $D = 0.8$, and $T_0 = \mu_{T_l}$.

clearly shows that the α_R values in case of the exponential model are greater than those obtained for the lognormal and Weibull models. As T_0 grows, the hazard rates for both lognormal and Weibull models increase while the hazard rate for the exponential model remains unchanged. This leads to almost similar seismicity at around $T_0 = 0.5\mu_{T_l}$ and thus to almost equal values of both Q_y and $\bar{Q}_y$ for all the three models (see Figures 8 and 9). Consequently, nearly equal values of α_R are obtained for the three models when $T_0 = 0.5\mu_{T_l}$ (see Figure 5). With further growth in the gap length, the hazard rates for both lognormal and Weibull models also increase leading to greater values of Q_y and even greater values of $\bar{Q}_y$, in comparison with the exponential model (see Figures 8 and 9). As a result, we obtain higher values for α_R at all time periods for both lognormal and Weibull models when $T_0 = \mu_{T_l}$ (see Figure 6). However, as mentioned earlier, the hazard rate increases at

DOI: 10.1002/eqe

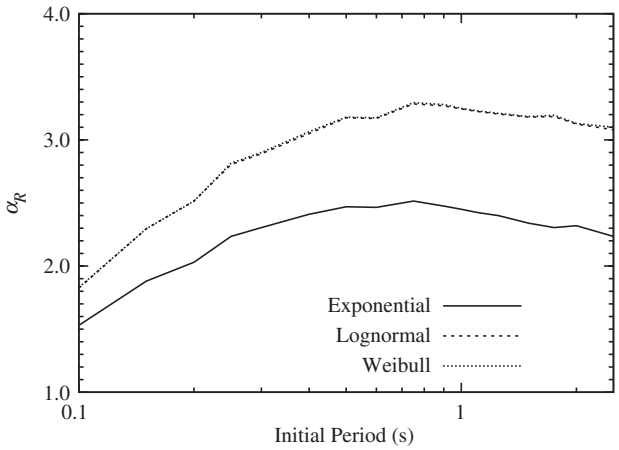

Figure 7. DFR spectra for different seismicity models in case of $\mu = 3$, $D = 0.8$, and $T_0 = 1.5\mu_{T_l}$.

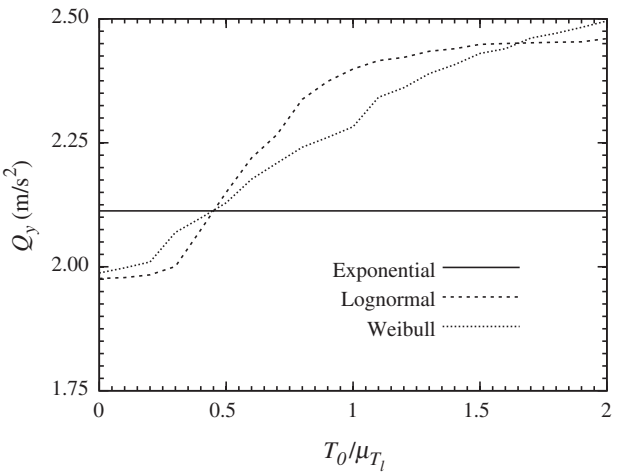

Figure 8. Variations of Q_y with T_0/μ_{T_l} for different seismicity models in case of $\mu = 3$, $D = 0.8$, and 0.3 s initial period.

a faster rate in case of the lognormal model and therefore, the lognormal model is associated with the largest α_R values at $T_0 = \mu_{T_l}$. With further increase in T_0, there is proportionately a smaller rise in the hazard rate for the lognormal model as it approaches its maximum. The hazard rate for the Weibull model on the other hand continues to rise. At $T_0 \approx 1.5\mu_{T_l}$, the hazard rates of both lognormal and Weibull distributions become almost equal (see Figures 8 and 9), and identical DFR spectra are obtained for the two models at $T_0 = 1.5\mu_{T_l}$ (see Figure 7). For $T_0 > 1.5\mu_{T_l}$, however, greater α_R values would be obtained for the Weibull model, while those will decline beyond certain value of T_0 in case of the lognormal model. It may be mentioned that the α_R values will

DOI: 10.1002/eqe

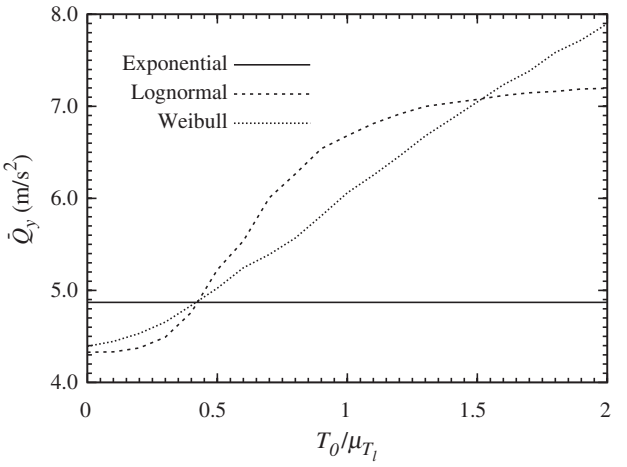

Figure 9. Variations of $\bar{Q}_y$ with T_0/μ_{T_l} for different seismicity models in case of $\mu = 3$, $D = 0.8$, and 0.3 s initial period.

not increase indefinitely (with T_0; in case of the Weibull model) due to the constraint on the maximum magnitude of expected earthquake events. α_R values are also bound by the R_μ values because yield strength levels approach the linear design levels with increase in α_R.

It is clear from the above discussion that it is the hazard rate that primarily determines which of the three seismicity models gives the most conservative estimates of DFR spectra. Greater this rate is, greater is the effect of higher order events on $\bar{Q}_y$ and then greater are the α_R estimates. There are three ranges of gap length, $T_0 < T_0^l$, $T_0^l < T_0 < T_0^u$, and $T_0 > T_0^u$, over which the exponential model, lognormal model and the Weibull model respectively give the most conservative estimates. The values of T_0^l and T_0^u are governed by the design life of the structure besides the parameters of the seismicity models. In the present case, T_0^l is about half the mean return period while T_0^u is about one and half times the mean return period.

5. CONCLUSIONS

In this study, the concept of DFR spectrum has been considered for designing a SDOF structural system so that it survives all earthquake events through its design life without having to undergo repairs after damaging events. DFR spectrum gives the factors for oscillators of different initial periods by which the yield strength levels should be raised (for a given amount of cumulative damage at the end of the design life) beyond those given by the conventional ductility-based design. Besides accounting for the effects of multiple events, these factors also account for the inherent disparities between the ductility-based and damage-based designs for single event. These factors depend significantly on the seismicity model used to estimate the rates of earthquake occurrences of different magnitudes, and therefore the effect of seismicity model on DFR spectrum has been studied in case of a hypothetical seismic environment.

Three seismicity models have been considered. For all three models, return periods are distributed exponentially for the events up to the magnitude of 7. However, for larger events (up to

DOI: 10.1002/eqe

a maximum magnitude of 8), return periods are assumed to follow exponential, lognormal and Weibull distributions. The key parameter that differentiates the three models and associated hazard rates is the seismic gap length or quiescent period, and it is found that it is the yield strength level in multiple-event design that is more sensitive to the hazard rate. More conservative DFR spectra can thus be obtained from each of the three models, depending on the value of the seismic gap length. Whereas for small gap lengths, it is conservative to use exponential model, for intermediate and large gap lengths, lognormal and Weibull models may be used respectively. In fact, it may be quite unconservative to assume the exponential model (for large events) in case of large gap lengths.

The calculations for DFR spectrum in this study have been based on several assumptions. Some of those including the use of equivalent linear oscillator and treatment of nonstationarity via transient transfer function at finite time are well-accepted in scientific literature. However, the use of equivalent linear oscillator to estimate second largest, third largest, etc. response peaks, the use of order statistics approach for estimating the magnitudes of the largest and other ordered events during the lifetime of the structure, and the use of Equations (26) and (27) to describe the strength and stiffness degradations during an event may be merely assumptions that have little consistency with the reality. Also, sequence of the occurrence of the damaging events has been so assumed as to obtain an upper bound of the cumulative damage in the oscillator. Despite these limitations, the results of this study are found to be broadly consistent with the known trends and may therefore mark a preliminary step in the direction of a more comprehensive 'no-repairs' performance-based design.

REFERENCES

1. Amadio C, Fragiacomo M, Rajgelj S. The effects of repeated earthquake ground motions on the non-linear response of SDOF systems. *Earthquake Engineering and Structural Dynamics* 2003; **32**:291–308.
2. Ballio G. European approach to design of steel structures. *Proceedings of Hong Kong Fourth World Congress*, Hong Kong 1990; 935–946.
3. Vidic T, Fajfar P, Fischinger M. Consistent inelastic design spectra: strength and displacement. *Earthquake Engineering and Structural Dynamics* 1994; **23**:507–521.
4. Gutenberg B, Richter CF. Earthquake magnitude, intensity, energy and acceleration. *Bulletin of the Seismological Society of America* 1942; **32**:163–191.
5. Cornell CA, Winterstein SR. Temporal and magnitude dependence in earthquake recurrence models. *Bulletin of the Seismological Society of America* 1988; **78**(4):1522–1537.
6. Esteva L. Geology and probability in the assessment of seismic risk. *Proceedings of Second International Congress*, *International Association of Engineering Geology*, San Paulo, Brazil, 1974.
7. Patwardhan AS, Kulkarni RB, Tocher DA. A semi-Markov model for characterizing recurrence of great earthquakes. *Bulletin of the Seismological Society of America* 1980; **70**(1):323–347.
8. Kiremidjian AS, Suzuki SA. A stochastic model for site ground motions from temporally dependent earthquakes. *Bulletin of the Seismological Society of America* 1987; **77**(4):1110–1126.
9. Nishenko SP, Buland R. A generic recurrence interval distribution for earthquake forecasting. *Bulletin of the Seismological Society of America* 1987; **77**(4):1382–1399.
10. Kagan YY. Statistics of characteristic earthquakes. *Bulletin of the Seismological Society of America* 1993; **83**(1):7–24.
11. Chen PS, Lin PH. An application of theory of extreme values to moderate and long-interval earthquake prediction. *Acta Geophysica* 1973; **16**:6.
12. Kijiko A, Sellovell MA. Triple-exponential distribution, a modified model for the occurrence of large earthquakes. *Bulletin of the Seismological Society of America* 1981; **71**:2097–2101.
13. Yegulalp TM, Kuo JT. Statistical prediction of the occurrences of maximum magnitude earthquakes. *Bulletin of the Seismological Society of America* 1974; **64**(2):393–414.

DOI: 10.1002/eqe

14. Gupta ID, Deshpande VC. Application of log-Pearson type-III distribution for evaluation of design earthquake magnitudes. *Journal of the Institution of Engineers* (*India*), *Civil Division* 1995; **75**:129–134.
15. Trifunac MD, Brady AG. A study on the duration of strong earthquake ground motion. *Bulletin of the Seismological Society of America* 1975; **65**:581–626.
16. Gupta ID, Trifunac MD. Defining equivalent stationary PSDF to account for nonstationarity of earthquake ground motion. *Soil Dynamics and Earthquake Engineering* 1998; **17**:89–99.
17. Trifunac MD, Lee VW. Preliminary empirical model for scaling Fourier amplitude spectra of strong ground acceleration in terms of earthquake magnitude, source to station distance, site intensity and recording site conditions. *Report No. CE 85-03*, Department of Civil Engineering, University of Southern California, Los Angeles, CA, U.S.A., 1985.
18. Trifunac MD, Brady AG. Correlation of peak acceleration, velocity and displacement with earthquake magnitude, distance and site conditions. *Earthquake Engineering and Structural Dynamics* 1976; **4**:455–471.
19. Caughey TK. Random excitation of a system with bilinear hysteresis. *Journal of Applied Mechanics* (ASME) 1960; **27**:649–652.
20. Gupta ID, Trifunac MD. Order statistics of peaks in earthquake response. *Journal of Engineering Mechanics* (ASCE) 1988; **114**(10):1605–1627.
21. Gupta VK. Developments in response spectrum-based stochastic response of structural systems. *ISET Journal of Earthquake Technology* 2002; **39**(4):347–365.
22. Kunnath SK, Reinhorn AM, Lobo RF. IDARC version 3.0: a program for the inelastic damage analysis of RC structures. *Report NCEER-92-2002*, National Center for Earthquake Engineering Research, State University of New York at Buffalo, New York, U.S.A., 1992.
23. Reinhorn AM, Kunnath SK, Mander JB. Seismic design of structures for damage control. In *Nonlinear Seismic Analysis and Design of Reinforced Concrete Buildings,* Fajfar P, Krawinkler H (eds). Elsevier Applied Science: London, 1992.
24. Todorovska MI. Comparison of response spectrum amplitudes from earthquakes with a lognormally and exponentially distributed return period. *Soil Dynamics and Earthquake Engineering* 1994; **13**:97–116.
25. Sykes LR, Nishenko SP. Probabilities of occurrence of large plate rupturing earthquakes for the San Andreas, San Jacinto, and Imperial faults, California, 1983–2003. *Journal of Geological Research* 1984; **89**:5905–5927.

DOI: 10.1002/eqe